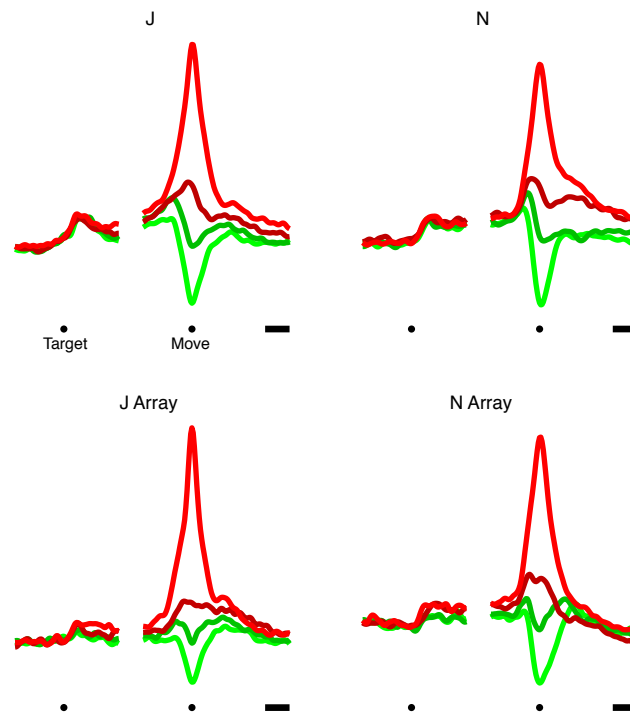
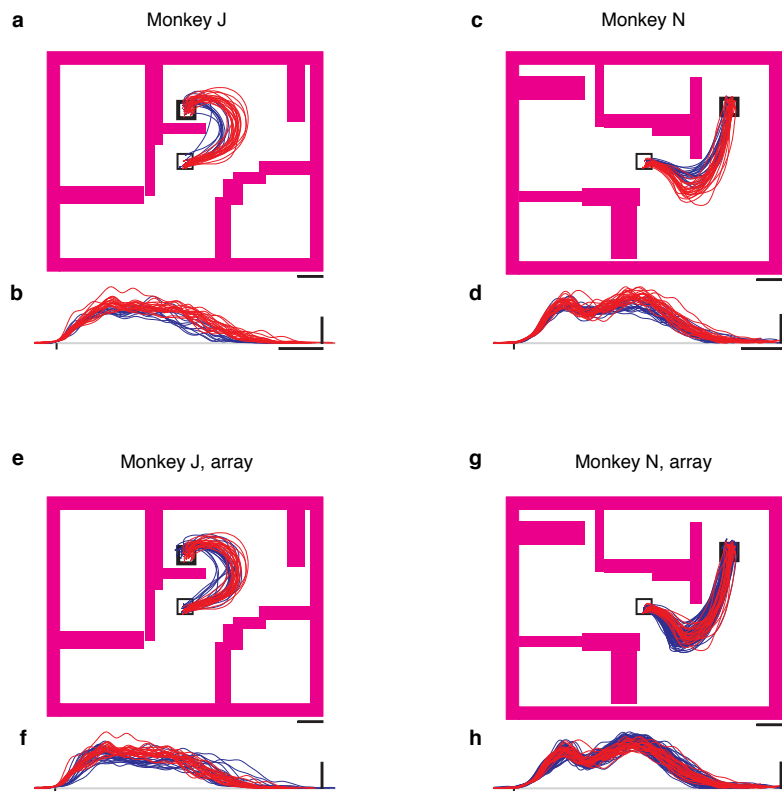


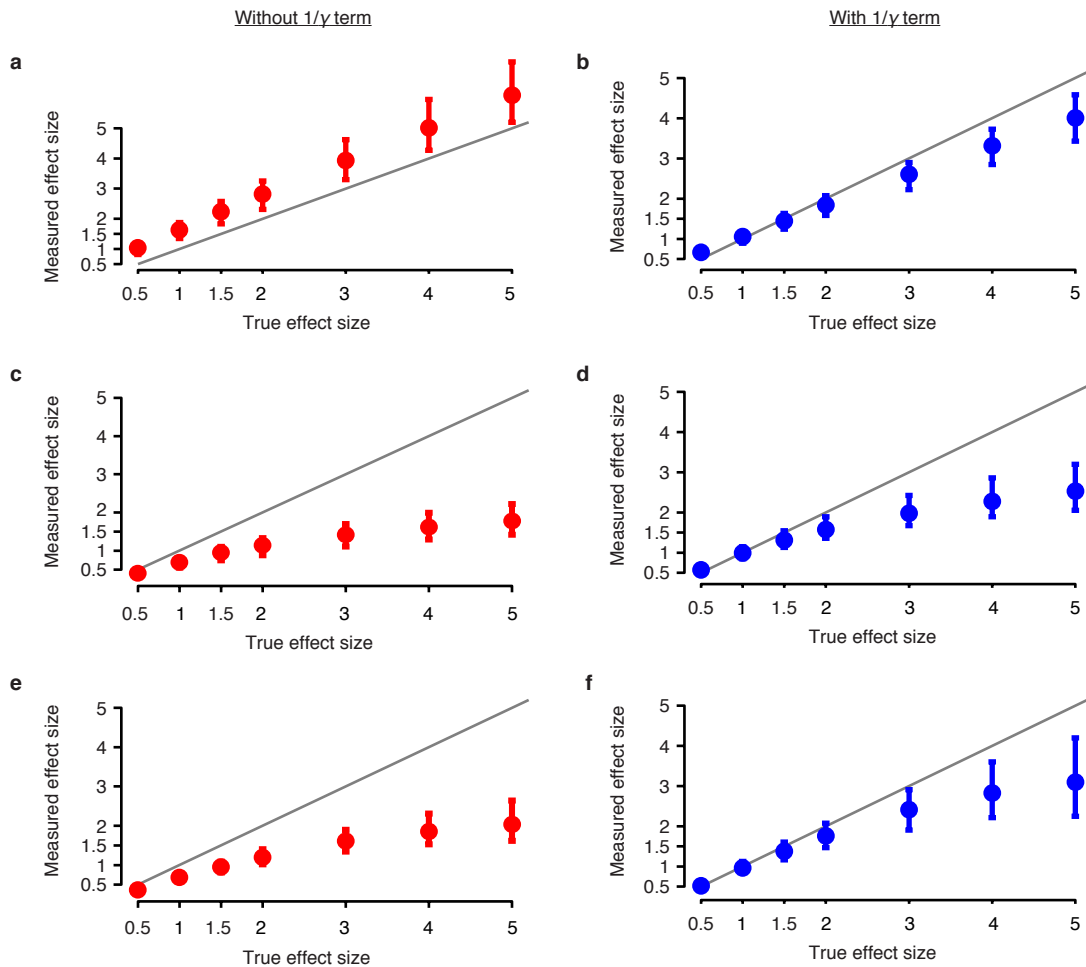
Supplementary materials for:
Cortical activity in the null space: permitting preparation without movement
Matthew T. Kaufman, Mark M. Churchland, Stephen I. Ryu, Krishna V. Shenoy



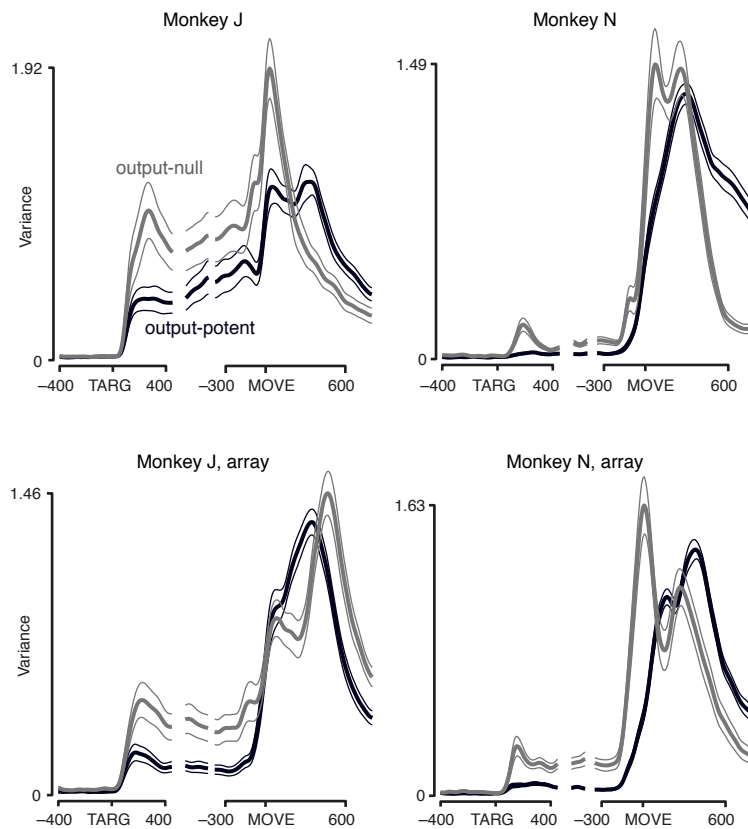
Supplementary Figure 1 Tuning is mismatched between the preparatory and movement epochs. Each panel represents firing rate data from one dataset. For each neuron, firing rates were first averaged over trials, then conditions were sorted based on the neuron's firing rate at movement onset. The reddest trace shows the average across neurons for each neuron's "most preferred" condition. The greenest trace shows the average across neurons for each neuron's "least preferred" condition; the other two traces represent the 33rd and 67th percentile conditions. Very little preparatory tuning remains after this procedure, indicating that tuning is mismatched between the preparatory and movement epochs. Each neuron's response was normalized by its range before averaging. Target, target onset; Move, movement onset. Scale bar indicates 200 ms.



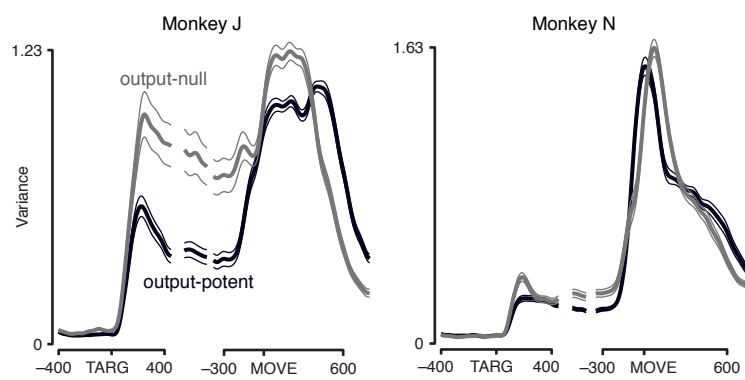
Supplementary Figure 2 Behavioral consistency within and across days. Single-electrode neural data were collected over many days, and it is important that behavior was similar over time. In particular, since EMG data were recorded late during single-electrode data collection, and array recordings were performed after that, this figure compares behavior during neural data collection and EMG data collection. **(a)** All reaches for a particular maze for dataset J (single electrode recordings for monkey J). Blue shows reaches made during one neuron worth of neural recording, red during one muscle worth of EMG recording. Note that some blue traces are hidden by the red traces. The same EMG session is shown as in Figure 1. The neural recording day was chosen to be the most distant possible from the EMG day, 4.5 months apart. Behavior for this example maze was slightly more different between days than typical. The scale bar is 40 mm. **(b)** The speed profile for each reach, aligned to movement onset (*black tick*). Colors as in **(a)**. Scale bars are 100 ms and 0.5 m/s. **(c-d)** Same for dataset N (single electrode recordings for monkey N). The days were again chosen to be maximally far apart, ~3 months. **(e-f)** Same for dataset JA (array recordings for monkey J). Days were 9.5 months apart. **(g-h)** Same for dataset NA (array recordings for monkey N). Days were 1.2 months apart.



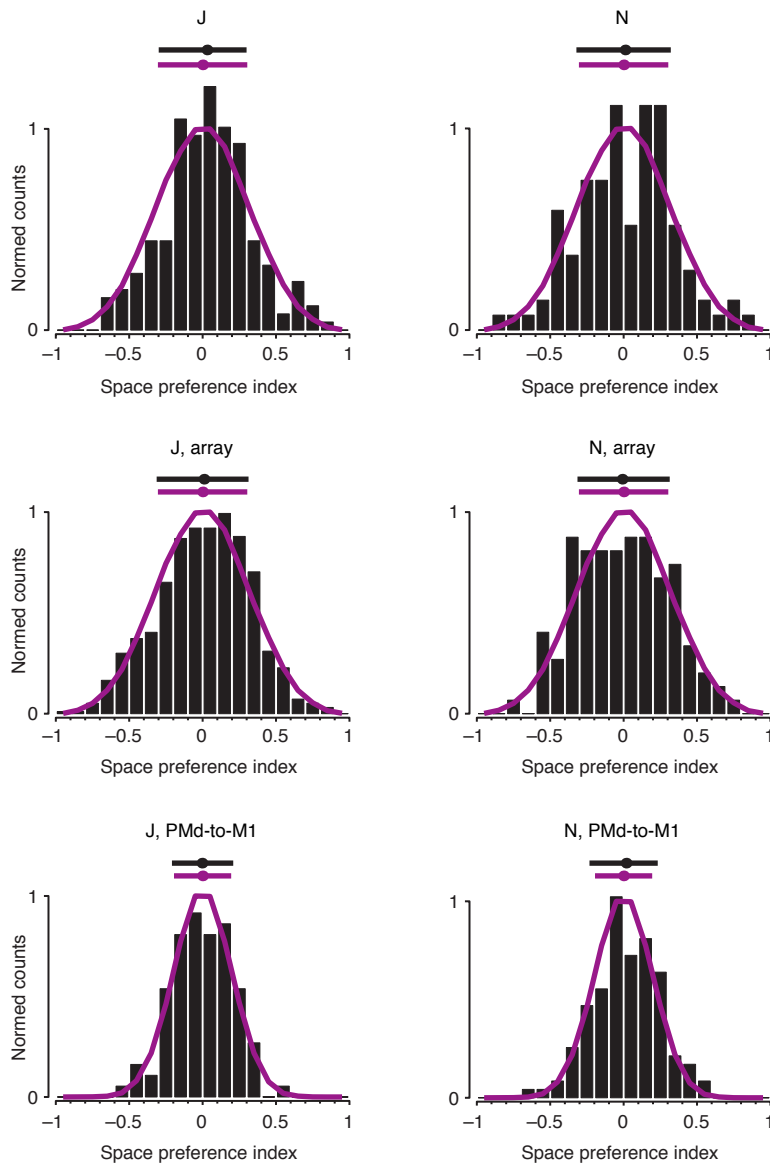
Supplementary Figure 3 Output-null method on additional simulated data. Plots are as in Figure 5. These plots illustrate algorithm performance when the simulated data contains unequal numbers of output-null and output-potent dimensions, and how the analysis performs with (*right*) and without (*left*) the $1/\gamma$ term. (**a-b**) Four output-potent dimensions and two output-null dimensions were present in the simulated data. The analysis assumed three and three. Though false positives were present without the $1/\gamma$ term (**a**), using the term prevented false positives (**b**). (**c-d**) Four output-null dimensions and three output-potent dimensions were present in the simulated data, but the analysis assumed three and three. Again, false positives are absent, and the $1/\gamma$ term helps to reduce underestimation of the effect size. (**e-f**) Three output-potent and six output-null dimensions were present in the simulated data. The analysis assumed three and three. We note that this situation, of having only a few output-potent dimensions and many output-null dimensions, is likely to be the true one. Here, again, the analysis produces reasonable results with a mild underestimation of the effect size.



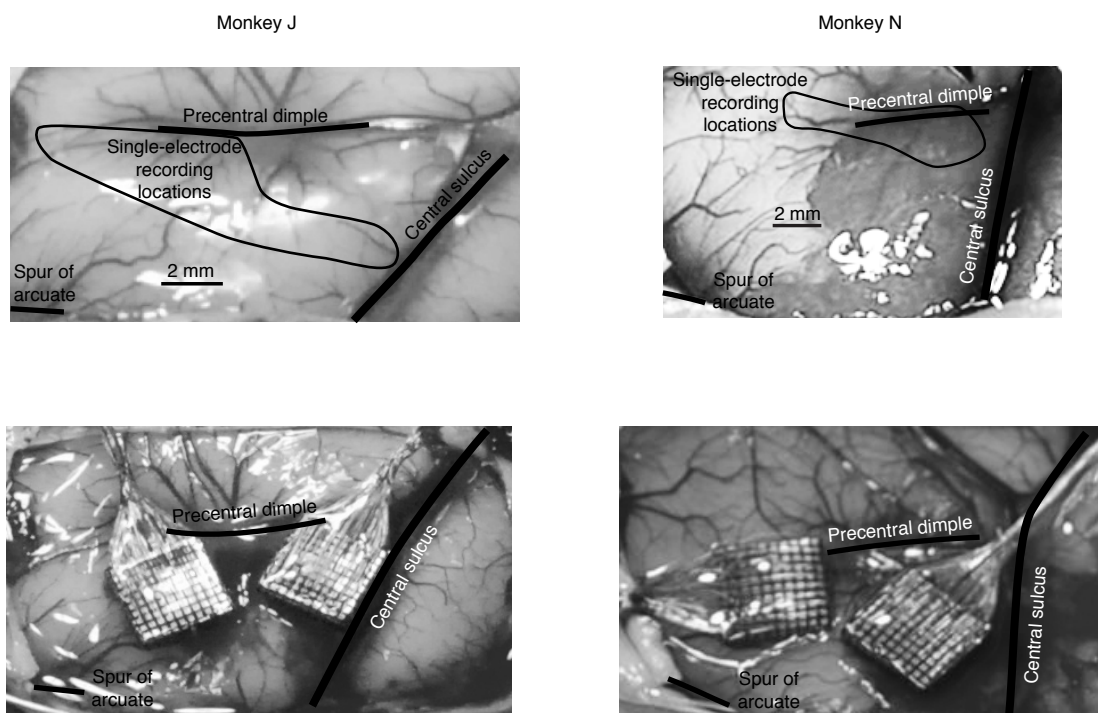
Supplementary Figure 4 Output-null results from cortex to muscles as a function of time. This figure is similar to Figure 4d, but shows all datasets and all time points. We measured the tuning depth at each time point in the putative output-null dimensions (*gray*) and output-potent dimensions (*black*). As predicted, in all four datasets, the tuning depth during preparation was greater in the output-null dimensions than in the output-potent dimensions. This confirms that during movement preparation, the pattern of activity preferentially avoids the dimensions that cause muscle activity. Importantly, however, the effects shown here are smaller than the effects shown in Figure 4c because the present analysis cannot factor in the shift in the across-condition mean that occurs at target onset. Note that here the variance across conditions is shown, which effectively squares the ratio of how strong movement-epoch tuning appears relative to preparatory tuning; preparatory activity thus looks weaker than it would in a PSTH. Flanking traces indicate s.e.m.s computed via resampling of conditions.



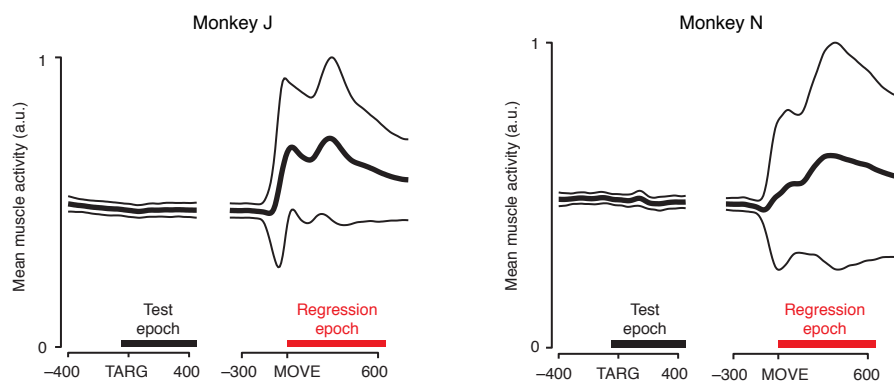
Supplementary Figure 5 Output-null results from PMd to M1 as a function of time. These plots are similar to Supplementary Figure 4, but show the output-null results for PMd to M1 instead of both areas to the muscles. Again, note that this analysis underestimates the true effect size because it cannot factor in the shift in the across-condition mean that occurs at target onset, which is a major source of the effect size especially for monkey N.



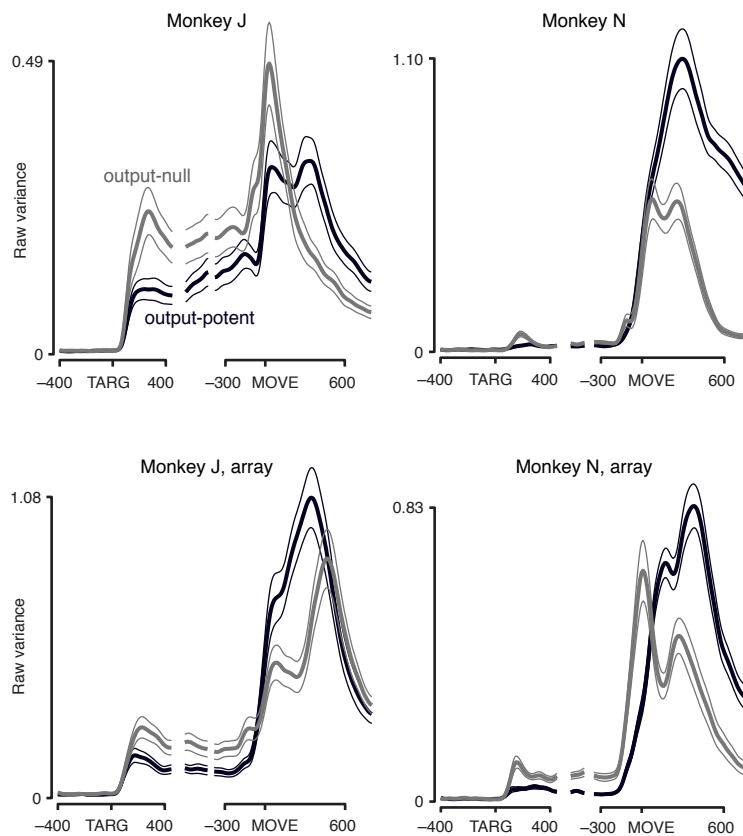
Supplementary Figure 6 Analysis of neurons' projections into the output-null and output-potent spaces. For each neuron, a space preference index was computed, which is +1 if the neuron contributes solely to output-potent dimensions and -1 if the neuron contributes solely to output-null dimensions. If there were two populations of neurons, where one population contributed mostly to output-potent dimensions and the other contributed mostly to output-null dimensions, we would expect a distribution with a peak near each extremum. The histogram of the values from the data are plotted in black, one panel per dataset. The null distribution (computed from random vectors in the same-dimensional space) is plotted in purple. One standard deviation above and below zero is plotted as horizontal bars above, with dots indicating the means. In each dataset, the empirical distribution is nearly identical to the random distribution. This indicates that there are not two separate populations of neurons driving the differences between the output-null and output-potent dimensions.



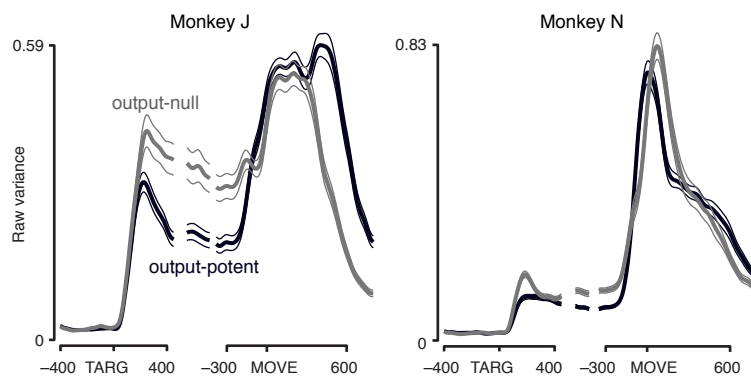
Supplementary Figure 7 Recording locations. *Left*, monkey J; *right*, monkey N. *Top panels* show outlines of the entry points where single-electrode recordings were made. Note that many recordings were made deep in the central sulcus, underneath the outlined areas. *Bottom panels* show the locations of the electrode arrays. For scale in the bottom panels, the arrays were square, 4.2 mm on a side.



Supplementary Figure 8 Muscle activity over time relative to key epochs. Plots as in Figure 7b, but for each monkey (J, *left*; N, *right*). Each muscle's activity was first normalized by its range (over all times and conditions). The *heavy trace* indicates the mean of these values across all muscles at each time point. This therefore gives a general idea of how average activity changed over time (muscle activity rose more strongly than it fell). To obtain an estimate of tuning depth with time, the standard deviation was taken across conditions (different reach shapes) at each time point for each normalized muscle. These values were then averaged across muscles at each time point. The width of the *thin traces* around the mean show this value, at one standard deviation. Muscle activity was only used in our main analysis to identify output-potent dimensions and output-null dimensions. To do so, we only used activity from the peri-movement epoch (*red bar*). Specifically, we used 0 to +650 ms from movement onset. Note that the muscle is already responding strongly by this time point. Effect size was computed using only preparatory data (*black bar*).



Supplementary Figure 9 Output-null results from cortex to muscles as a function of time, without the $1/\gamma$ term. These plots are similar to the plots in Supplementary Figure 4, but the tuning in each space has not been normalized by the movement-epoch tuning. The $1/\gamma$ term was important in simulations to produce accurate results, and we therefore believe that Supplementary Figure 4 represents the most quantitatively interpretable effect sizes. However, we wished to show that the central effect was not somehow created by normalization. The current analysis demonstrates that the central effect survives without the $1/\gamma$ term. Again, note that this analysis underestimates the true effect size because it cannot factor in the shift in the across-condition mean that occurs at target onset. This limitation appears to be particularly important in the monkey N dataset.



Supplementary Figure 10 Output-null results from PMd to M1 as a function of time, without the $1/\gamma$ term. These plots are similar to Supplementary Figure 5, but as in Supplementary Figure 9, the values are not normalized by the movement-epoch tuning. Again, note that this analysis underestimates the true effect size because it cannot factor in the shift in the across-condition mean that occurs at target onset, which is a major source of the effect size in monkey N.

Supplementary Tables

Supplementary Table 1. Output-null effect of each brain area separately to the muscles.

Dataset	PMd to muscles		M1 to muscles	
	Tuning ratio	p-value	Tuning ratio	p-value
J	2.476	0.011*	0.994	0.581
N	4.891	0.053	2.069	0.091
JA	2.484	0.012*	2.067	0.021*
NA	1.832	0.184	2.530	0.121
Geometric mean	2.725		1.811	

Significant values starred. Most half-datasets did not have enough statistical power to reach significance, but 7/8 exhibited the expected greater-than-unity tuning ratio. It is not clear which area by itself “should” exhibit stronger effects, since preparatory activity is presumably reduced stepwise from PMd to M1 to the muscles (PMd has stronger preparatory activity, and M1 is more strongly connected to the muscles). In the data, there may be a trend for effects in PMd to be stronger than in M1, though we did not have the statistical power to resolve any such difference. One sub-dataset, M1 from dataset J, exhibits a vanishing and non-significant wrong-direction effect.